

**Development of Optically Enhanced Back Reflectors and
Improved Deposition Processes for Amorphous Silicon-
Based Photovoltaic Technologies**

ANNUAL TECHNICAL STATUS REPORT
June 15 2003 - June 15 2004

Scott J. Jones (Principal Investigator), J. Doehler, Masat Izu
Tongyu Liu, David Tsu, Jeff Steele and Rey Capangpangan
Energy Conversion Devices, Inc.

NREL Technical Monitor
Bolko von Roedern

Prepared under Subcontract No. ZDJ-2-30630-22

Preface

This Annual Subcontract Report covers the work performed by Energy Conversion Devices, Inc. for the period June 15, 2002 to September 15, 2003 under DOE/NREL Subcontract No. ZDJ-2-30630-22. The following personnel participated in the research program.

R. Capangpangan, J. Doehler, M. Izu, S. Jones, T. Liu, S.R. Ovshinsky, J. Steel and D. Tsu.

We would like to specially thank Professor Hellmut Fritzsche for the many discussions and input he has made in advancing this program.

Executive Summary

Objectives

In this program, we plan to improve the module efficiencies through development of a new optically enhanced Al/ZnO back reflector and improved i-layer deposition process. In the case of the back reflector development, a multi-layered thin film structure consisting of films with contrasting indices of refraction placed between the Al and ZnO layers of the back reflector will be developed to improve the reflectivity of the back reflector structure. The ultimate goal is to achieve the high currents and cell efficiencies typically obtained with the Ag/ZnO back reflector with a new optically enhanced back reflector that can be used in the solar module products. Ag/ZnO back reflectors are presently used only in R&D applications due to long term instabilities related to electromigration of Ag. For the multi-layered structure, focus will be on preparing the layers using sputtering techniques so that this technology might be quickly applied to ECD's present back reflector fabrication process that uses sputtering techniques.

In the case of the i-layer, focus will be on preparing microcrystalline silicon based intrinsic layers for low cost, high stable efficiency solar cells through the use of high intensity (decomposition rate) plasmas. In these studies, the effects of such deposition conditions as ion bombardment, substrate temperature and etchant gases on the grain size and film transparency will be studied and correlated with cell performance.

Achievement of the goals of this program and application of these advancements to ECD's joint venture company's production lines would lead to an immediate improvement in module efficiencies. These advances along with ECD's participation in the NREL a-Si teams with other development programs will contribute to the ultimate goal of achieving stable efficiencies of 15% using a low-cost, scalable, manufacturable techniques and inexpensive substrates.

Approach

To improve the back reflector performance, a new multi-layer Al/(low index layer)/(high index layer)/(low index layer)/ZnO structure is being developed in this program. Fabrication of the back reflector layers is initially being done using the dc sputtering technique presently used in Uni-solar's production plant. As a first step to development of the back reflector structure, a number of materials are being developed. In particular, deposition conditions for a transparent conductor with an index of refraction of 1.6 or less is being devised. We are first testing different ZnO alloys as a low index material with ZnOMgF and ZnOSi alloys already developed. Also the conditions used to make the high index materials ($n > 3.0$) are being determined with doped a-Si and a-SiGe as the first two candidates.

Having developed the necessary materials, a number of Al/(low index layer)/(high index layer)/(low index layer)/ZnO structures are being made to optimize the reflectivity of the stack through variation of the layer thicknesses. Low bandgap a-SiGe nip semiconductor stacks will be deposited on the back reflector structures followed by top TCO/Al contacts to fabricate small area solar cells to test device performance. With these cells, we will be looking for improvements in short circuit currents and cell efficiencies with the use of these new types of back reflector structures. Besides testing for reflectivity, we will also test the use of different

layer texturing schemes to obtain light scattering properties which enhance the probability of photon absorption and increase the short circuit currents.

Microwave techniques are being used to prepare microcrystalline Si nip cells to achieve high performance at i-layer deposition rates near 15 Å/s. This is a continuation of previous studies in which 7.0% stable efficiencies were obtained for single-junction cells using these high deposition rates. The i-layers are presently being made in a single chamber system while the doped layers are prepared by the standard 13.56 MHz PECVD technique in a second multi-chamber system. Deposition conditions are being varied to optimize small area cell performance.

Results/Status

The following has thus far been achieved during this program:

Year 1.

- 1) A sputtering machine was refurbished to complete the back reflector depositions,
- 2) Conditions were developed to make transparent, conductive ZnO layers with index of refraction values near 1.8,
- 3) Conditions were developed to make transparent, conductive ZnOSi and ZnOMgF alloys with index of refraction values between 1.6 and 1.7,
- 4) Al/ZnO/ZnOSi/doped Si/ZnOSi/ZnO back reflector structures were initially tested and optimized for high reflectivity in the 600-1000nm wavelength range (the range of interest for back reflectors).
- 5) Use of different SiH₄+SiF₄ total gas flows during microcrystalline Si i-layer depositions were tested to increase the degree of etching during growth but no improvement in cell performance was obtained.

Year 2.

- 1) Al/ZnO/ZnOSi/doped Si/ZnOSi/ZnO back reflector structures were optimized and high reflectivity values in the 600-1000nm wavelength range, similar to those for Ag/ZnO structures, were obtained.
- 2) Using new Si deposition conditions to prepare Al(specular)/ZnO/ZnOSi/Si/ZnOSi/ZnO back reflector stacks and textured top ZnO layers, a 7% improvement was obtained for the short circuit currents of a-SiGe single-junction cells.
- 3) Through the use of post deposition annealing treatments, we have fabricated ZnOMgF materials with n<1.6, high transparency and high conductivities values.

Publications

Listed below are articles in which these works were published during the entire program.

S.J. Jones, G. Demaggio, J. Doehler, T. Liu and D. Tsu, "Development of Optically Enhanced Back Reflectors for Amorphous Silicon-Based Photovoltaic Technologies.", Program and Proceedings: NCPV and Solar Program Review Meeting 2003, March 24-26, Denver, CO, 823.

S. J. Jones, D. Tsu, T. Liu, J. Steele, R. Capangpangan and M. Izu, "Development of transparent conductive oxide materials for improved back reflector performance for amorphous silicon based solar cells." Proc Mat. Res. Soc. Spring 2004, to be published.

Table of Contents

Title Page	1
Preface	2
Executive Summary	3
Table of Contents	5
List of Figures	6
List of Tables	7
Introduction	8
Experimental	10
Results	11
Back Reflector Studies	11
Increasing the index of refraction for sputtered a-Si	15
Further development of low n materials	17
Microcrystalline Si studies	19

List of Figures

Figure 1. ECD/United Solar's triple-junction solar cell structure.	8
Figure 2. Cell structure using the new type of back reflector.	9
Figure 3. Depiction of dc sputtering system.	10
Figure 4. Test structures used for optimizing back reflectors.	10
Figure 5. New back reflector structure.	11
Figure 6. Reflectance spectra for various structures.	14
Figure 7. Index of refraction at $\lambda=850\text{nm}$ vs. band gap energy for sputtered a-Si.	15
Figure 8. Reflectance data for back reflectors made using old and new Si deposition recipes.	16
Figure 9. Quantum efficiency plots for a-SiGe cells with different back reflectors. The Al/ML/ZnO is an Al(specular)/ZnO/ZnOSi/Si/ZnOSi/ZnO structure with a thick top ZnO layer.	16
Figure 10. Resistivity vs. index of refraction at $\lambda=850\text{nm}$ for ZnO alloys.	18
Figure 11. SEM photos for a) ZnO (200K Magnification), b) ZnOMgF (200K Magnification), c) ZnO (100K Magnification), and d) ZnOMgF (200K Magnification).	18

List of Tables

Table I. a-SiGe cell performance for devices made with different back reflectors.	12
Table II. a-SiGe cell performance for devices made with different back reflectors. (Specular Al)	13
Table III. a-SiGe cell performance for devices made with different back reflectors (Thick and Thin ZnO)	13
Table IV. IV data for a-SiGe cells with different back reflectors (with and without multi-layer structure).	17
Table V. Data for $\mu\text{c-Si}$ cells made using old and new systems.	20

Introduction

Over the past 15 years [6-8], ECD has pioneered and continued the development of several key a-Si PV technologies. An a-Si/a-SiGe/a-SiGe triple junction, spectrum splitting cell structure has been developed to achieve high efficiencies for a-Si based solar modules. This structure is depicted in Figure 1. With this design, ECD and United Solar have set several light-to-electricity efficiency records including United Solar's world record 10.5% stable triple junction a-Si alloy solar panel with over 1 ft² area and a 13% stable active area efficiency for a 0.25 cm² cell. To market this technology, a roll-to-roll manufacturing process was developed through ECD's machine division. This inexpensive process uses a 14", ½ mile long steel web as a substrate material on which the light absorbing layers is deposited. ECD has developed the process through several generations of manufacturing machines with the out come of a production process which offers significant economy-of-scale advantages and results in dramatic cost savings as the volume of production increases. This technology is presently being used in United Solar's 25 MW production line in Auburn Hills, MI.

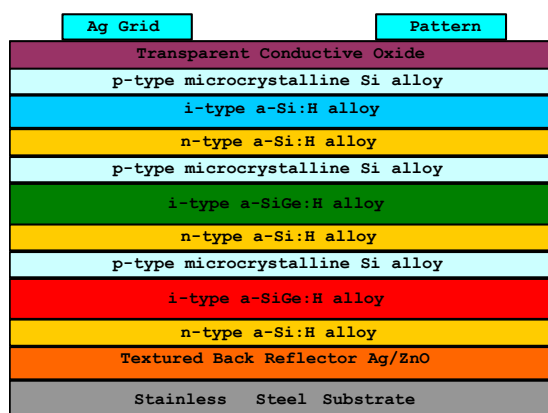


Figure 1. ECD/United Solar's triple-junction solar cell structure.

While several advances have been made on the R&D level to increase small area cell and module efficiencies, the stable efficiencies presently obtained for the large area modules made in Uni-Solar's production machine are between 8.0 and 8.5%, roughly 20% lower than the 10.5% value obtained for the 1 sq. ft. module in R&D. The deficiencies in the module performance in production are in part related to the following alterations to the fabrication process from that used in R&D:

- 1) Use of deposition rates of 3 Å/s as compared with the 1 Å/s rate used in R&D – in order to use gas utilization rates which make the process economically feasible, conditions must be used that increase the i-layer deposition rates to roughly 3 Å/s. This leads to poorer i-layer and cell performance.
- 2) Use of Al/ZnO back reflectors rather than the Ag/ZnO used in R&D – because of poor long term yield issues, the Ag/ZnO layer is not presently used in production, instead a sturdier Al/ZnO structure is used. Because of the poorer reflectance

properties of Al as compared with Ag, roughly a 10% drop in current and cell efficiency is observed with the use of the Al/ZnO back reflector.

In terms of addressing these issues in order to improve the module efficiencies obtained in production, several research and development programs have been undertaken. To improve the performance of cells made using i-layer deposition rates of 3-10 Å/s, both United Solar and ECD, through the Thin Film Partnership Program, have carried out studies of i-layers made at high rates using the standard 13.56MHz PECVD technique and VHF PECVD techniques using frequencies between 70 and 100 MHz[9,10]. While some progress has been made, the efficiencies for the cells made at the higher deposition rates remain lower than those made using the 1 Å/s conditions.

In contrast to the high deposition rate issue, little work has recently been done on improving the back reflector used in the manufacturing of the solar modules. Considering the potential 10% increase in module performance if an environmentally stable back reflector that has similar performance capabilities to Ag/ZnO is developed, it is important that some research efforts be undertaken in this area. Some attempts have been made to using barrier layers to improve the stability of the Ag/ZnO back reflectors[4]. While some short term improvement of the cell yields have been observed, the long term air exposure issue has yet to be solved without substantial decreases in cell efficiency.

As part of this NREL supported program, we plan to improve the currents of the modules through development of a new optically enhanced Al/ZnO based back reflector. In the case of the back reflector development, a multi-layered thin film structure consisting of films with contrasting indices of refraction (n) placed between the Al and ZnO layers of the back reflector will be developed (See Figure 2). The addition of the multi-layer structure will improve the reflectance properties of the back reflector. In this program, these new types of back reflectors will be tested in amorphous silicon based single junction and multi-junction devices. The differences in n of the different layers of the multi-layered back reflector and electrical conduction through the multi-layered structure will be optimized to obtain the highest reflection values, highest currents and best cell performance. The ultimate goal is to achieve the high currents and cell efficiencies typically obtained with the Ag/ZnO back reflector with an Al/(multi-layered structure)/ZnO back reflector that can be used in the solar module products. For the multi-layered structure, focus will be on preparing the layers using sputtering techniques so that this technology might be quickly applied to ECD's present back reflector fabrication process that uses sputtering techniques.



Figure 2. Cell structure using the new type of back reflector.
Experimental

For the back reflector development, the layers were primarily made using the dc sputtering technique. The system used to prepare the layers is depicted in Figure 3. This deposition reactor contains four different sputtering cathodes to deposit four different types of materials in one system pumpdown. A movable substrate and rail system are used to move the substrate past the targets at a fixed speed during film deposition to simulate the roll-to-roll deposition process. Presently, back reflector layers are deposited on six 2" x 2" substrates during each run, however substrates as large as 1' x 1' can be used with the existing hardware. During materials development, films were deposited on 7059 glass and/or quartz substrates for various optical and electrical measurements to determine such properties as reflectivity, conductivity, index of refraction, absorption and film thicknesses. To fabricate the Si layer, a P doped Si target (200ppm) was used while a ZnAl alloy target with 5% Al was used to fabricate the ZnO alloys.

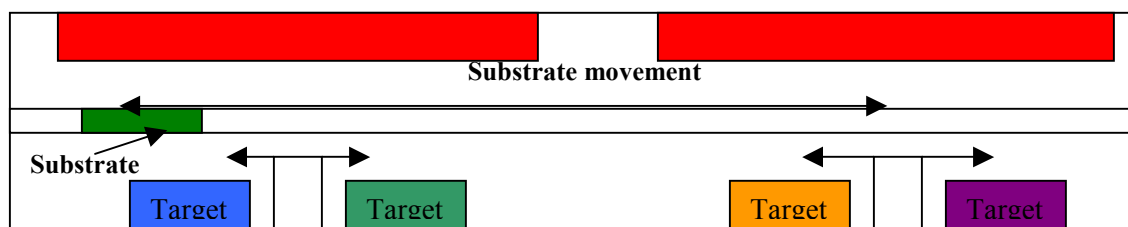


Figure 3. Depiction of dc sputtering system.

For multi-layer back reflector fabrication, multi-layer stacks were deposited on 5 mil stainless steel substrate typically used in Uni-solar's manufacturing facility. To initially characterize the back reflector performance, nip amorphous silicon germanium semiconductor structures were deposited on the back reflectors followed by top contacts to create 0.25 cm² solar cells (depicted in Figure 4). The nip structures were fabricated using a research scale, multi-chamber load locked deposition system and the standard 13.56 MHz Plasma Enhanced Chemical Vapor Deposition (PECVD) technique. Both the ITO and Al layers are prepared using standard evaporation techniques. For promising back reflector conditions, a-Si:H/a-SiGe:H/a-SiGe:H triple-junction cells will be made.

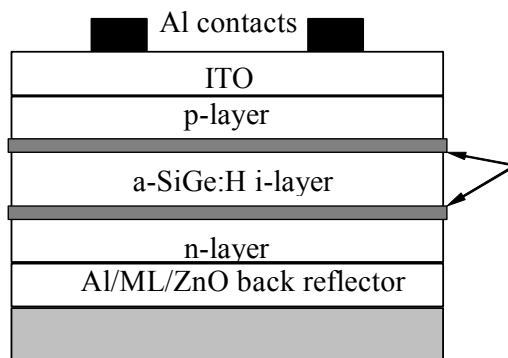


Figure 4. Test structures used for optimizing back reflectors.

To characterize the solar cells, standard IV and spectral response (quantum efficiency) measurements are made. Since our goal is to use the back reflectors to enhance the currents for the a-SiGe:H middle and bottom cells in the triple-junction cells, the AM1.5 light for the IV measurements of the a-SiGe:H cells is filtered using 630nm cutoff filters to simulate the absorption due to a top a-Si:H cell. To complete light soaking studies, the cells are subjected to 600-1000 hrs. of one sun light with the cell temperature fixed at 50°C. The i-layer thicknesses are determined using standard capacitance techniques.

For the microcrystalline Si growth studies, single-junction nip microcrystalline Si solar cells are being fabricated to characterize the microcrystalline Si quality. The Si materials have been prepared using microwave techniques to achieve high decomposition and growth rates. Since our goal is to create cells for red-light absorption, cells are again characterized using unfiltered AM1.5 light and AM1.5 light filtered using 630nm cutoff filters to complete IV measurements. Light soaking of the cells are also completed using the method used for the a-SiGe:H cells for the back reflector characterization.

Results

Back Reflector Studies

The multi-layer structure to be optimized in this program is depicted in Figure 5. The multi-layer consists of a high index conductive material ($n = 3.2$ or greater) sandwiched between two low index materials ($n < 2.0$). Both of the materials need to be somewhat transparent and conductive. Early results from modeling of the reflectivity suggest that more focus should be spent on developing the low index material than increasing the index of the high index materials. From modeling the optical properties for the stack, it was determined that lowering n for the two low n layers would be more effective in increasing the reflection from the back reflector than raising the index of refraction for the high n material. Thus we have spent the initial portion of this program developing the low index, transparent conductive oxide. As figure 5 shows, we have chosen to initially use doped a-Si as the high index material because of minimal light absorption in the red portion of the solar spectrum, a reasonably high conductivity when doped, and an index of refraction of roughly 3.2.

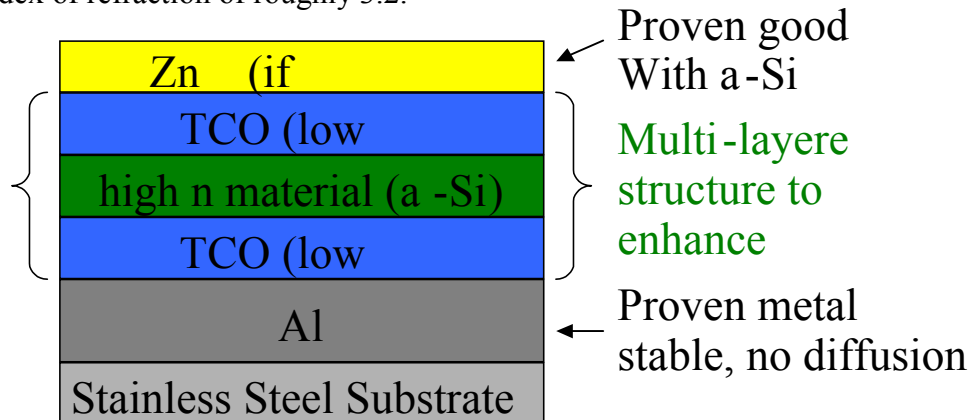


Figure 5. New back reflector structure.

In devising the new back reflector structure, one should consider two properties the present Ag/ZnO back reflectors provide. First is the high reflectivity of the Ag metal and second is the texture surface at the ZnO top surface which provides light scattering properties to enhance the probability of light collection and higher solar cell currents. The textured surface is typically obtained by using high deposition temperatures during metal growth and/or thick layers (metal and/or ZnO). With the new Al/ML/ZnO structure, the addition of the multi-layered structure should lead to enhanced reflectivity. The exact source for light scattering (surface texturing or particle scattering) in this new back reflector structure has yet to be determined.

In the last annual report, we presented results on the use of the Al/ML/ZnO back reflector in a-SiGe bottom cells in which the multi-layer (ML) consisted of a ZnO/ZnOSi/Si/ZnOSi structure. The results are shown in Table I. The Al layers for these back reflectors were prepared at either low substrate temperatures to obtain a specular surface or at high temperatures to obtain a textured surface. Comparing the cells with Al/ML/ZnO having textured Al to those with specular Al, the cell current and overall performance is significantly higher for the cells with the textured Al surface. This demonstrates the improvement one is able to obtain with the textured surface. Comparing the performance of the Al/ML/ZnO back reflector having the textured Al with Al/ZnO structures made using both the R&D and Production machines, the overall performance is quite similar. There are some differences in the V_{oc} , J_{sc} , FF and R_s values, but the P_{max} values are all in the 2.5-2.7 mW/cm² range. The 2-3 Ohms cm² difference in the series resistance for the Al/ML/ZnO and the Al/ZnO may suggest a slight problem with the Al/ML/ZnO back reflector, however the difference may also reflect slight variations in the Ge contents in the i-layers. The performance of the Al based back reflectors are still significantly poorer than that for the Ag/ZnO back reflectors, as is shown in the table.

Table I.
a-SiGe cell performance for devices made with different back reflectors.
Cell properties obtained using AM1.5 light filtered with 630nm cutoff filter.
(ML structure is ZnO/ZnOSi/Si/ZnOSi/ZnO)

Type of Back Reflector	V_{oc} (V)	J_{sc} (mA/cm ²)	FF	R_s (Ohms cm ²)	P_{max} (mW/cm ²)
Al/ML/ZnO (Textured Al)	0.519	9.47	0.527	14.5	2.59
Al/ML/ZnO (Textured Al)	0.538	9.05	0.527	15	2.57
Al/ML/ZnO (Specular Al)	0.538	7.03	0.511	18.9	1.93
Al/ZnO (Textured Al)	0.520	9.50	0.545	12.1	2.69
Al/ZnO (Textured Al)	0.509	9.29	0.538	12.2	2.54
Ag/ZnO (Textured Ag)	0.573	11.4	0.541	13.6	3.53
Ag/ZnO	0.556	11.4	0.515	18.4	3.26

(Textured Ag)					
---------------	--	--	--	--	--

The fact that no improvement in the back reflector performance was seen with the addition of the ML when an Al textured surface is used may be a result of the fact that 1) the textured surface minimizes the effect of the ML, 2) the modeling results are incorrect and a larger difference in n between the high n (ZnOSi) and low n materials (Si) is needed, or 3) the properties of the materials we are using for the ML structure differ from what we expect. To minimize the effect of texturing, we prepared a series of Al/ZnO back reflectors using low substrate temperatures during Al growth to minimize the surface texture. Table II compares average IV properties for a-SiGe cells made using these back reflectors to those made using Al/ML/ZnO structures, again with a specular Al surface. The a-SiGe nip structures were made under nominally the same deposition conditions which are different from those used to make the cells whose data is shown in Table I. One can see that the performance for the cells made using the Al/ML/ZnO is similar to those without the ML structure. Thus the ML structure initially did not improve the cell performance even when the Al surface is not textured.

Table II.
a-SiGe cell performance for devices made with different back reflectors.
Cell properties obtained using AM1.5 light filtered with 630nm cutoff filter.
(ML structure is ZnO/ZnOSi/Si/ZnOSi/ZnO)

Type of Back Reflector	V_{oc} (V)	J_{sc} (mA/cm ²)	FF	R_s (Ohms cm ²)	P_{max} (mW/cm ²)
Al/ZnO (Specular Al)	0.533	7.09	0.551	19.2	2.08
Al/ML/ZnO (Specular Al)	0.546	6.92	0.563	18.3	2.13

As an alternative to texturing the Al surface to enhance the cell currents through light scattering, we have tested the effect of texturing the top ZnO layer by using very thick top layers. Table III compares data for a-SiGe cells with Al/ML/ZnO that have thin (standard) and thick ZnO layers. While the ZnO thickness has yet to be fully optimized, a significant increase in performance is seen with the thicker ZnO. Thus when the ML structure is optimized, texturing the ZnO layer rather than the Al layer is an option that will be further tested.

Table III.
a-SiGe cell performance for devices made with different back reflectors.
Cell properties obtained using AM1.5 light filtered with 630nm cutoff filter.
(ML structure is ZnO/ZnOSi/Si/ZnOSi/ZnO)

Type of Back Reflector	V_{oc} (V)	J_{sc} (mA/cm ²)	FF	R_s (Ohms cm ²)	P_{max} (mW/cm ²)
Al/ML/ZnO - Thin ZnO (Specular Al)	0.546	6.92	0.563	18.3	2.13
Al/ML/ZnO - Thick ZnO	0.562	7.89	0.576	14.3	2.55

(Specular Al)

Having eliminated the textured surface as the source for the lack of improvement with the use of the ML structure, we have recently reexamined the properties of each of the layers in the ML structure. Figure 6 compares reflectivity data for four different structures, 1) a single Al layer made in the same dc sputtering system used to make the ZnO alloys, 2) Al/ZnO/ZnOSi/Si/ZnOSi/ZnO, and 3) Al/MgF₂/Si/MgF₂. For structures 2 and 3, the layer thicknesses were varied to obtain the highest reflection in the region of interest (600-100nm) where light is absorbed by the bottom and middle component cells of the triple-junction a-Si/a-SiGe/a-SiGe structure. The Al//MgF₂/Si/MgF₂ structure was made in an earlier program with the MgF₂ layers made using evaporation techniques. It was demonstrated that this stack has similar reflectivity properties to specular Ag/ZnO in the 600-100nm region. In this region, one can see that on average the reflectance for the Al/ZnO/ZnOSi/Si/ZnOSi/ZnO structure is slightly lower than that for the bare Al. This was unexpected since modeling suggested that the structure would lead to improved total reflectance. The lower values for the Al/ZnO/ZnOSi/Si/ZnOSi/ZnO structure could be related to some source of absorption that has yet to be determined or a textured surface (interface) which would lead to a scattering source not taken into account by our modeling. Thus, lower than expected reflectance values are likely limiting the solar cell performance.

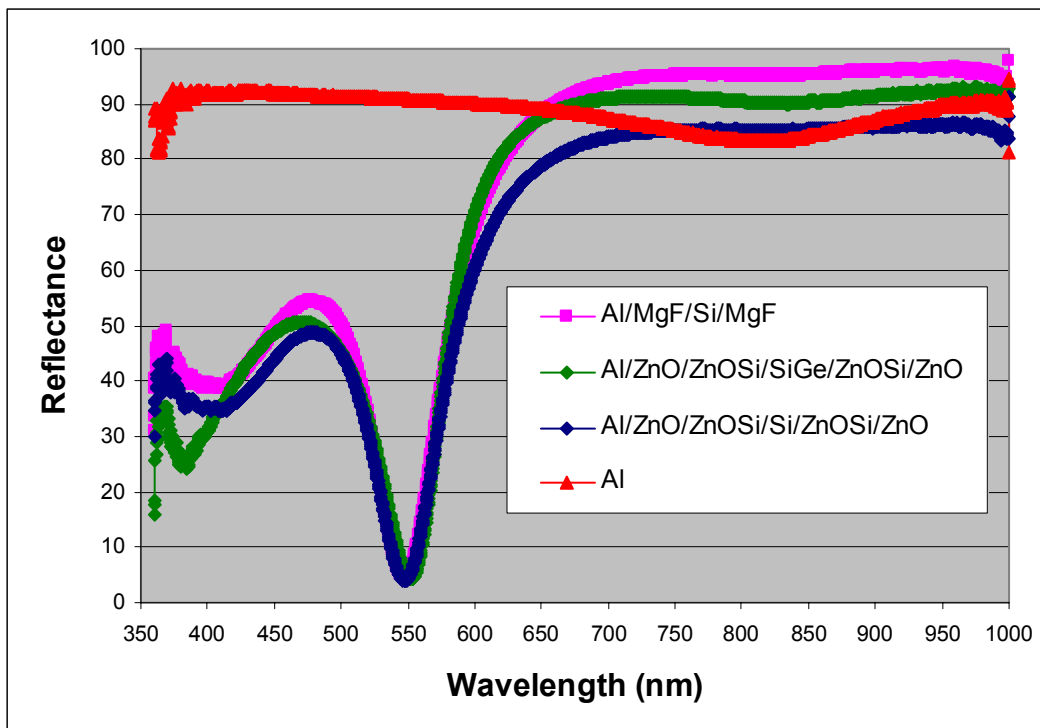


Figure 6. Reflectance spectra for various structures.

To improve the reflectance of the Al/ML/ZnO structures, single layer component films were deposited onto 7059 glass and quartz substrates for optical measurements in the visible

region of the light spectrum to revisit the material properties. The ZnOSi and ZnO layers had similar properties to those previously obtained with the index of refraction for the ZnOSi layers being 1.64. Surprisingly, we discovered that the Si made by sputtering had an index of refraction between 2.6 and 2.8, significantly lower than the 3.2 value previously obtained using the same deposition procedure. This difference in index between the expected 3.2 value and the actual 2.6-2.8 values could explain why we aren't observing an improvement in back reflector performance with the addition of the ML structure. The sputtering target used to make these layers is heavily doped with P and we believe that the level of doping may be changing through the thickness of the target and that we are now making more heavily doped films with open microstructures.

Increasing the index of refraction for sputtered a-Si

In an effort to increase n for the a-Si, we prepared a number of single layer Si films under a variety of conditions and measured their optical properties. In Figure 7, n at 850nm is plotted as a function of the bandgap of the material (E_g). The bandgaps were determined by fitting the optical data using the Tauc-Lorentz method. The wide range in E_g demonstrates that both amorphous and nanocrystalline Si films were made. To achieve a bandgap near 1.6 eV and $n > 3.4$, higher power conditions than those previously used were required as well as higher hydrogen flows and higher substrate temperatures. Values ≥ 3.6 for n were only obtained for materials with E_g less than 1.4 eV, thus having a significant fraction of nanocrystalline material. The high n value is desirable however the lower bandgap for the films with nanocrystallites made lead to increased red light absorption even with the lower absorption coefficient for the crystallites.

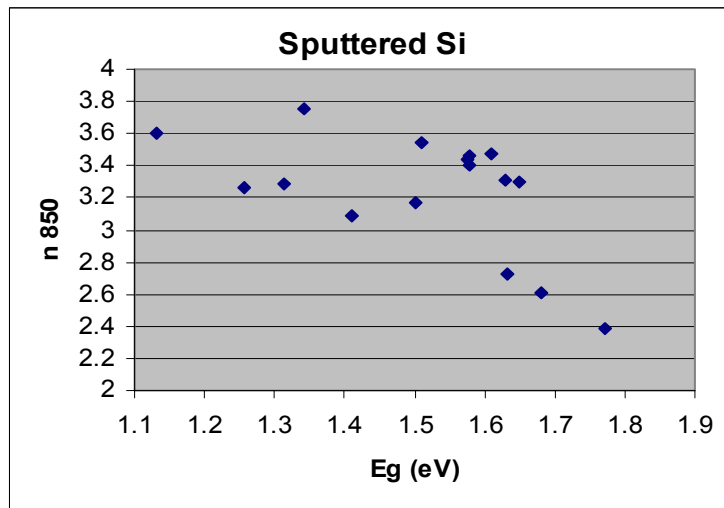


Figure 7. Index of refraction a $\lambda=850$ nm vs. band gap energy for sputtered a-Si.

We have used these Si materials with $n=3.4$, $E_g=1.6$ eV to make Al/ML/ZnO structures. Reflectance data for these film structures are compared with data for the Al/ML/ZnO made with the previous (old) Si conditions which led to films with low n in Figure 8. A significant improvement in the reflectivity in the red portion of the spectrum can be seen with the use of the

new Si deposition conditions. In fact, the reflectance below 700nm is quite similar to that for the Al/MgF₂/Si/MgF₂ structure and thus the Ag/ZnO back reflectors.

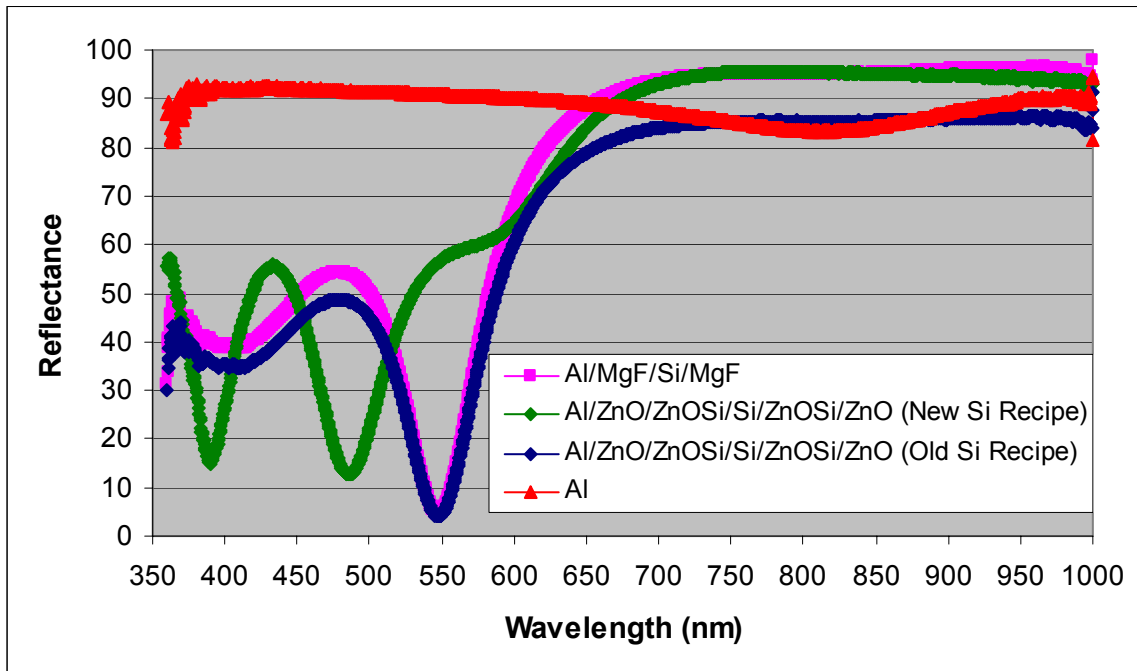


Figure 8. Reflectance data for back reflectors made using old and new Si deposition recipes.

Using the new Si deposition conditions to prepare Al(specular)/ZnO/ZnOSi/Si/ZnOSi/ZnO back reflector stacks and textured top ZnO layers, a 7% improvement was obtained for the short circuit currents of a-SiGe single-junction cells. Figure 9 below shows the improved quantum efficiency curves for a-SiGe bottom cells made with Al/Multi-layer/ZnO back reflectors compared with cells with Al/ZnO back reflectors made under nominally identical conditions. This improvement was obtained without full optimization of the film thicknesses and higher currents should be obtainable. The IV data for these cells in Table IV clearly shows the increase in short circuit current (calculated from the quantum efficiency data) caused by the increased red light response provided by the multi-layered back reflector. However, the gain in red light cell efficiency with the addition of the multi-layer stack is not as large as expected due to higher series resistances and lower fill factors that accompany the use of this multilayer stack.

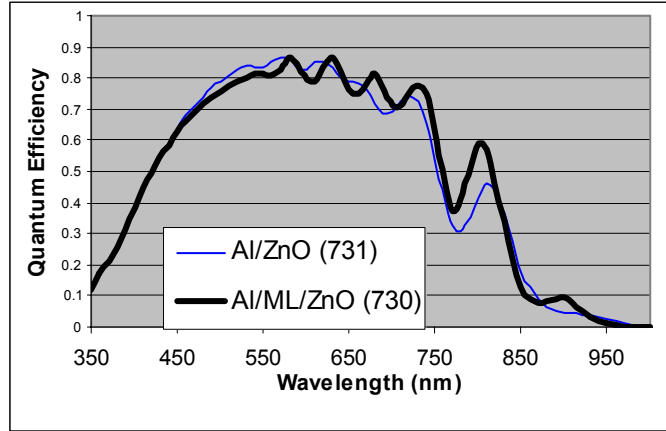


Figure 9.
Quantum efficiency plots for a-SiGe cells with different back reflectors. The Al/ML/ZnO is an Al(specular)/ZnO/ZnOSi/Si/ZnOSi/ZnO structure with a thick top ZnO layer.

Table IV.
IV data for a-SiGe cells with different back reflectors.
IV data taken using filtered AM1.5 light using 630 nm cutoff filter.

Type of Back Reflector	Voc (V)	Jsc (mA/cm ²)	FF	Rs (ohmcm ²)	Pmax (mW/cm ²)
Al/ZnO	0.593	8.94	0.524	17.2	2.78
Al/Multi-layer/ZnO	0.601	9.62	0.493	23.6	2.85

The higher series resistances for the Al/ML/ZnO back reflectors are likely associated with the conductivities of the ZnOSi or Si layers. Further improving the conductivities of the ZnOSi or Si layers materials may come through 1) making the Si layer under microcrystalline conditions rather than amorphous, 2) increased doping of the Si layer with transition metals like Ni, and 3) doping of the ZnOSi with F or Ni. These potential solutions will all be tested in the coming months.

Further development of low n materials

For both the ZnOSi and ZnOMgF materials, we have been able to prepare oxides with $n > 1.6$ with good transparency and high conductivity. However, for materials with $n \leq 1.6$, the resistivity values are significantly higher than those for the lower n materials as can be seen from the data in Figure 10. This quarter, we have subjected these materials with $n \leq 1.6$ to various post deposition treatments including high and low temperature anneals under various different atmospheres (air, N₂, vacuum, etc.) and UV light exposures. After each treatment, the optical and electrical properties of the films were measured. For the ZnOSi films, little or no changes in the material properties were observed after a variety post deposition treatments. In contrast, with a combination of treatments we have been able to decrease the resistivity of ZnOMgF films (see data in Figure 10) without significantly changing the index of refraction and no change in the transparency of the films. We will experiment further with the post treatments and also try to incorporate the treatments into the multi-layer growth process.

Considering these results, replacement of the ZnOSi alloys with ZnOMgF layers in the Al/ML/ZnO structure may lead to solar cells with lower series resistances and higher efficiencies.

Tests with the use of these materials in multi-layer back reflector stacks will be done in the coming months. Some effort will also be made in varying the processing temperature used in making the ZnOMgF films to see if the post annealing steps can be replaced with higher temperature processing.

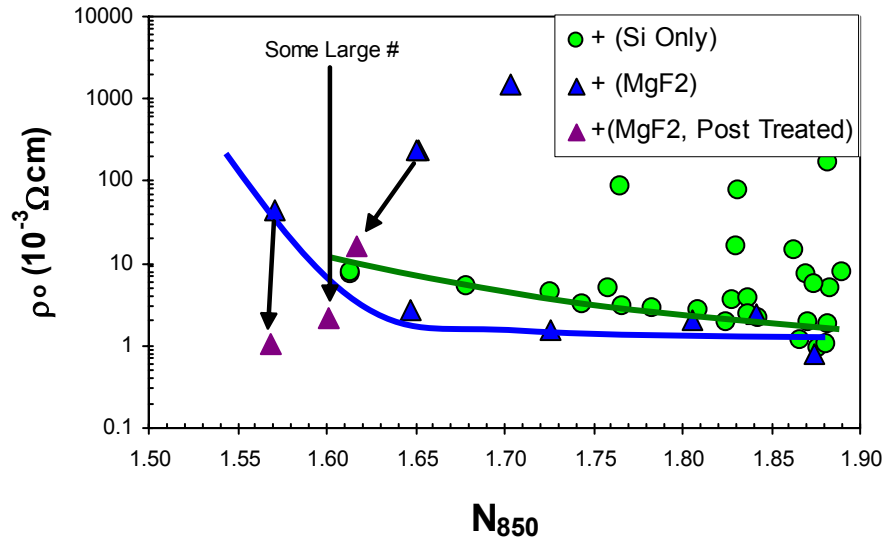


Figure 10. Resistivity vs. index of refraction at $\lambda=850\text{nm}$ for ZnO alloys.

Scanning Electron Microscopy (SEM) and Electron Dispersion Spectroscopy (EDS) measurements were also completed on certain alloys to determine composition as well as film surface morphology. SEM photos of ZnO and ZnOSi displayed virtually no change in the surface morphology with the addition of Si. In contrast, as the amount of MgF_2 was increased, the film was observed to be smoother with the structure having finer grains as can be seen in Figure 11. EDS also showed that the ZnOSi films with $n_{850}=1.6-1.7$ contain roughly 14 at.% Si while the ZnOMgF with similar n_{850} have 12 at.% Mg and 33 at.% F. The fact that the ZnOSi and ZnOMgF alloys only contain 12-14% Si and Mg and that SiO_2 and MgF_2 have n values of 1.6-1.7 suggests that besides alloying, low density regions and/or voids are forming with the addition of Si, Mg and F lowering the average value for n . The formation of the low density regions and/or voids could be responsible, at least in part, to the slight increase in resistivity noted with alloying. Measurements such as Small-Angle X-ray Diffraction have yet to be done to determine the size and shapes of these low density regions.

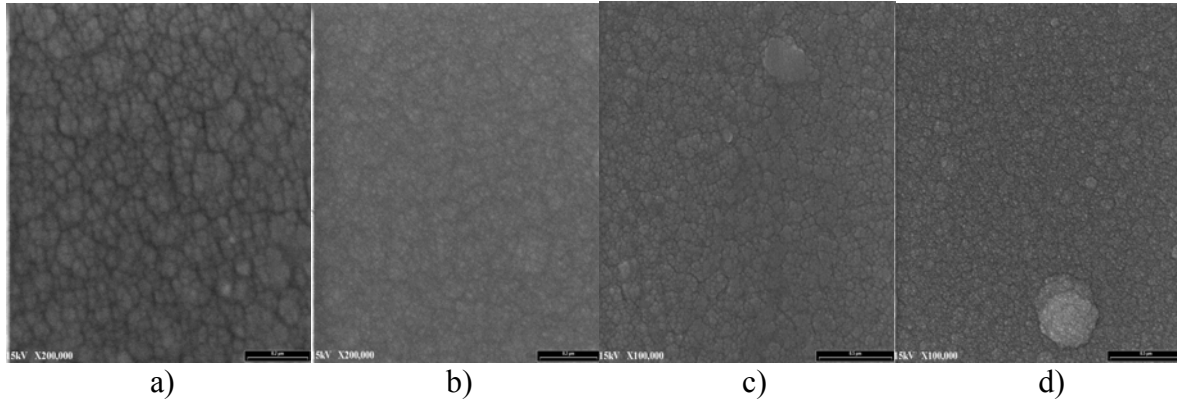


Figure 11.

SEM photos for a) ZnO (200K Magnification), b) ZnOMgF (200K Magnification), c) ZnO (100K Magnification), and d) ZnOMgF (200K Magnification).

Microcrystalline Si studies

Improving the performance of the back reflectors used for the solar panels fabricated with our machines is presently one of the major goals of ECD. Also other members of the team are developing the microcrystalline Si cells while little work is being done on the back reflector issue. Thus in this program we are focusing on the back reflector development and are spending less time on the microcrystalline Si development. During this reporting period, we have fabricated some microcrystalline Si single-junction cells in a new chamber attached to multi-chamber system in an attempt to improve the performance of the cells fabricated at high i-layer deposition rates (15-20 Å/s) over the efficiencies obtained in previous studies. The doped layers were deposited in a separate chamber using the same system and the standard 13.56MHz technique with deposition rates near 1 Å/s. The nip structures were deposited on Ag/ZnO coated stainless steel substrates and ITO/Al were deposited on top of the nip structures to complete the solar cell structures.

Table V compares data from our previous studies (8/01) with the studies completed in this program. The old system used to complete nano/microcrystalline Si depositions consisted of a single chamber and doped layers were fabricated in a different system. Thus films were exposed to air in between intrinsic and doped layer depositions. With the old system, we were able to obtain red light efficiencies of 2.8-2.9 mW/cm² using a technique in which a Gas Jet was subjected to high intensity microwaves. Using the new system, we have thus far been able to make microcrystalline i-layers at 5 Å/s, as compared with 15-20 Å/s made in the old system. Raising the deposition rates should likely come through increased SiH₄ flows. For the cells made using the 5 Å/s rate, we have achieved initial red light cell efficiencies of 3.0-3.1 mW/cm². These higher efficiencies with the new system are in part due to the lower deposition rates but may also be related to the elimination of the air break between doped and intrinsic layer depositions. However the efficiencies for the cells made using the new system degrade as a function of time as can be seen from the data in Table V. This is in contrast to the cells made using the old single chamber system which displayed no signs of degradation and were stable even after 2 years of air exposure.

This degradation of the cell properties is similar to what was found by others including Uni-solar with nano/microcrystalline solar cells and is due to the formation of a porous microstructure which allows oxygen diffusion and incorporation into the Si films. Thus in the

next year, we will be altering our deposition conditions to change the film microstructure to eliminate oxygen incorporation as well as increase the deposition rate.

Table V.
Data for $\mu\text{c-Si}$ cells made using old and new systems.
IV data taken using AM1.5 light filtered with 630nm cutoff filter (red light).

System	Time of exposure	V_{oc} (V)	J_{sc} (mA/cm ²)	FF	R_s (ohmcm ²)	P_{max} (mW/cm ²)
Old	2 years	0.483	10.32	0.570	8.1	2.84
Old	2 years	0.475	10.92	0.559	7.8	2.90
Old	2 years	0.452	11.47	0.528	7.8	2.74
Old	2 years	0.458	11.70	0.514	8.4	2.75
New	1 hour (Cell #1)	0.445	11.58	0.607	6.6	3.13
New	24 hours (Cell #1)	0.426	9.94	0.597	7.8	2.53
New	1 hour (Cell #2)	0.432	11.82	0.588	6.6	3.01
New	24 hours (Cell #2)	0.411	9.96	0.575	7.9	2.35